ELSEVIER

Earth and Planetary Science Letters 155 (1998) 205–219

EPSL

Mineral-magnetic proxies of erosion/oxidation cycles in tropical maar-lake sediments (Lake Tritrivakely, Madagascar): paleoenvironmental implications

D. Williamson [a,*,1], A. Jelinowska [b], C. Kissel [c], P. Tucholka [b], E. Gibert [d], F. Gasse [d], M. Massault [d], M. Taieb [a], E. Van Campo [a], K. Wieckowski [e]

[a] *Centre National de la Recherche Scientifique, CEREGE, BP 80, F-13545 Aix-en-Provence Cedex 4, France*
[b] *Département de Géodynamique et de Géophysique, Université Paris-Sud, F-91405 Orsay Cedex, France*
[c] *Centre des Faibles Radioactivités, CEA / CNRS, avenue de la Terrasse, F-91198 Gif-sur-Yvette Cedex, France*
[d] *Laboratoire d'Hydrologie et de Géochimie Isotopiques, Université Paris-Sud, F-91405 Orsay Cedex, France*
[e] *Institute of Geography and Special Organization, Polish Academy of Sciences, Warsawa, Poland*

Received 22 July 1997; revised 7 November 1997; accepted 21 November 1997

Abstract

Mineral-magnetic measurements were performed on the upper 16 m of five piston-cored sedimentary sequences from Lake Tritrivakely, Madagascar. AMS ^{14}C dating and correlation of the five magnetic susceptibility records allowed establishment of a composite sedimentary record of the last 46 kyr. Our data suggest that mineral-magnetic changes result from changes in concentration of strongly ferrimagnetic terrigenous minerals and from preservation/dissolution cycles of detrital iron oxides (primarily high-coercivity Fe(III) phases such as hematite) in alternately oxic and anoxic depositional environments. High-coercivity iron oxide phases are restricted to stratigraphic intervals that are interpreted to represent dry periods with oxic conditions. Comparison with other paleoenvironmental proxies (pollen, total organic carbon, lithology) suggests that the sediments record relatively humid conditions before 22 kyr BP, and relatively dry conditions during the Last Glacial Maximum (LGM) and the early Holocene. Such results contrast with the previous observations of relatively dry glacial conditions and humid mid-Holocene conditions in the summer rainfall area of East and SE Africa. © 1998 Elsevier Science B.V.

Keywords: Sediment magnetism; maar; lake; early diagenesis; paleoclimate; late quaternary; lolocene; madagascar

* Corresponding author. Present address: Department of Geology and Geophysics, 212 Pillsbury Hall, 310 Pillsbury Drive, Minneapolis, MN 55455, USA. E-mail: willi194@gold.tc.umn.edu

[1] Present address: Department of Geology and Geophysics, and Institute of Rock Magnetism, University of Minnesota, 100 Union Street SE, Minneapolis, MN 55 455, U.S.A.

PII S0012-821X(97)00217-3

1. Introduction

Numerous mineral-magnetic studies of lake sediments have shown the potential of magnetic methods to provide detailed records of regional climate (e.g., [1,2]). In maar-lake sediments from Europe, comparative studies of magnetic, pollen, and sedimentological data suggest that glacial/interglacial changes strongly modulate the input of primary Ti-iron oxides to the sediment [3]. In tropical areas, preliminary studies of volcanogenic sediments from Africa also suggest close relationships between climate and magnetic mineral assemblages [4,5]. In contrast to middle-latitude lakes, strong contributions of hematite from highly weathered oxisols resulted in the presence of magnetic mineralogical contrasts during alternating arid/humid climates [6].

In this paper, we have investigated the mineral-magnetic properties of a late Quaternary sedimentary sequence from Lake Tritrivakely (LT; 19°47′S,

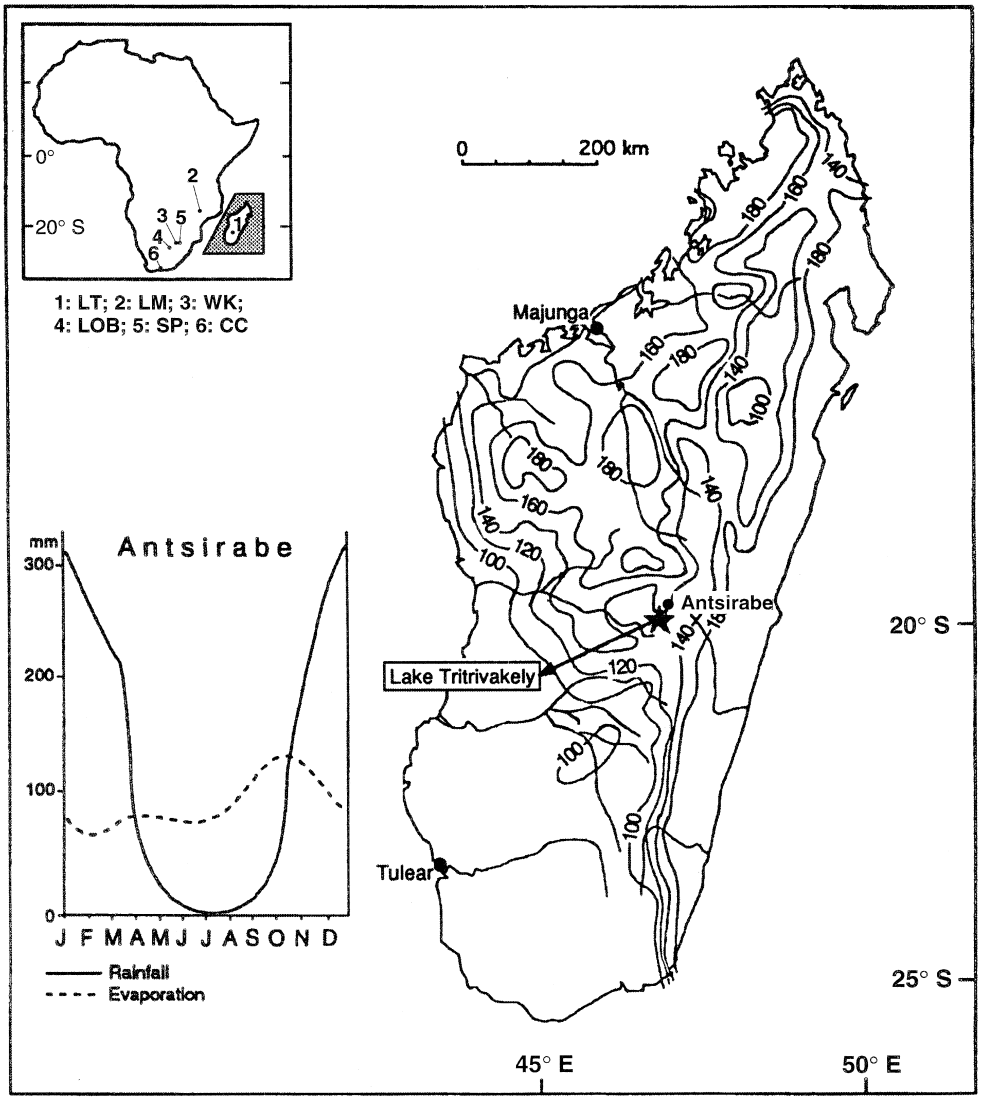

Fig. 1. Location map of Lake Tritrivakely with mean annual rainfall (cm). *Insets* show the location of Madagascar with other sites from southeast Africa (see text), and annual rainfall and evaporation at the town of Antsirabe [8].

46°55′E, 1778 m), a shallow basaltic maar-lake from the Ankaratra volcanic chain in central Madagascar (Fig. 1). The aim of this study is to determine the cause of mineral-magnetic changes by comparing magnetic data to other paleoenvironmental proxies, and to compare the LT paleoenvironmental record with other regional paleoclimate data.

2. General setting

The LT phreatomagmatic crater consists mainly of basaltic tuff-ring products that were strongly eroded and altered during long-term weathering which affected most of the Ankaratra volcanics [7,8]. The volcanic rocks provide a source of detrital Fe(III)-(oxyhydr)oxides such as titanomagnetite, maghemite, hematite and goethite. Owing to shallow water depths (0.5–3 m at the interannual scale), the modern lake is occupied by a *Cyperaceae* peat-bog which has dominated since the middle Holocene[9]. The regional tropical montane climate (16°C mean annual temperature; 1500 and 850 mm for mean annual rainfall and evaporation, respectively) is characterized by warm, humid summers under the influence of the northwest monsoon. In contrast, winters are dry and cool (the rainfall from April to October amounts to only 2–10% of the total annual rainfall) [8]. These climatic features suggest that paleoenvironments in the LT basin may have been strongly influenced by past summer monsoon circulations.

3. Coring and sampling

Five piston cores were collected in 1992 at the center of the LT crater by using two manual coring techniques: the Wright piston corer (core LT, 1 m sections to a depth of 13 m) and the Wieckowski piston corers (1 or 2 m sections to depths of: core T-I, 12.84 m; T-II, 40.03 m; T-III, 32.31 m; and T-IV, 14.74 m). The cores were extruded and sealed before

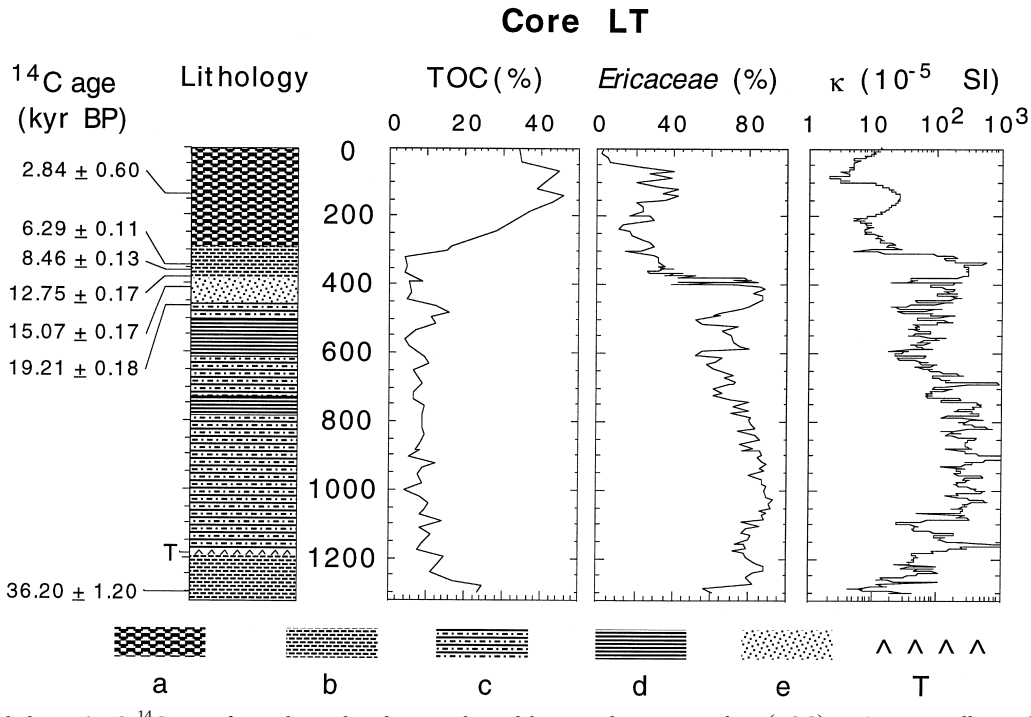

Fig. 2. Lithology, AMS ^{14}C ages from charcoal and macrophyte debris, total organic carbon (TOC), *Ericaceae* pollen and magnetic susceptibility (κ) for core LT. Lithologies are: a = *Cyperaceaea* peat; b = organic mud; c = coarsely laminated clayey mud; d = finely laminated organic–clayey mud; e = silt and sand; T = tephra layer.

transportation to the CFR core repository at Gif-sur-Yvette, France. The upper 16 m of the cored sedimentary sequence were subsampled in all cores for a wide range of studies including sedimentology, organic and isotopic geochemistry, AMS ^{14}C dating, diatom and pollen and rock-magnetic studies [10].

The cores were split lengthwise and sampled with plastic ''U-channels'' which were pushed into the center of each successive sub-section. Additional subsamples were taken for hysteresis measurements: 100–200 mg bulk sediment samples were collected at 5 or 10 cm intervals and were dried immediately under an argon atmosphere at 40°C to minimize laboratory oxidation.

4. Lithology and ^{14}C chronology

The upper 16 m of LT sediments consist of six dominant facies [10] (Figs. 2 and 3): (a) upper *Cyperaceae* peat which contains > 30% total organic carbon (TOC) at 2.5–0 m; (b) organic muds (up to 30% TOC) near the bottom of the sequence (15.5–14.8 m; 13–12.5 m) and immediately below the upper *Cyperaceae* peat (3.2–2.5 m); (c) clayey to silty muds, partly laminated (d), with (e) interbedded centimeter-bedded sand layers between 4.7 and 3.8 m; (T) a tephra layer (11.7 m).

Sixteen AMS ^{14}C dates were obtained from organic matter: 10 on fragments of *Cyperaceae* leaves,

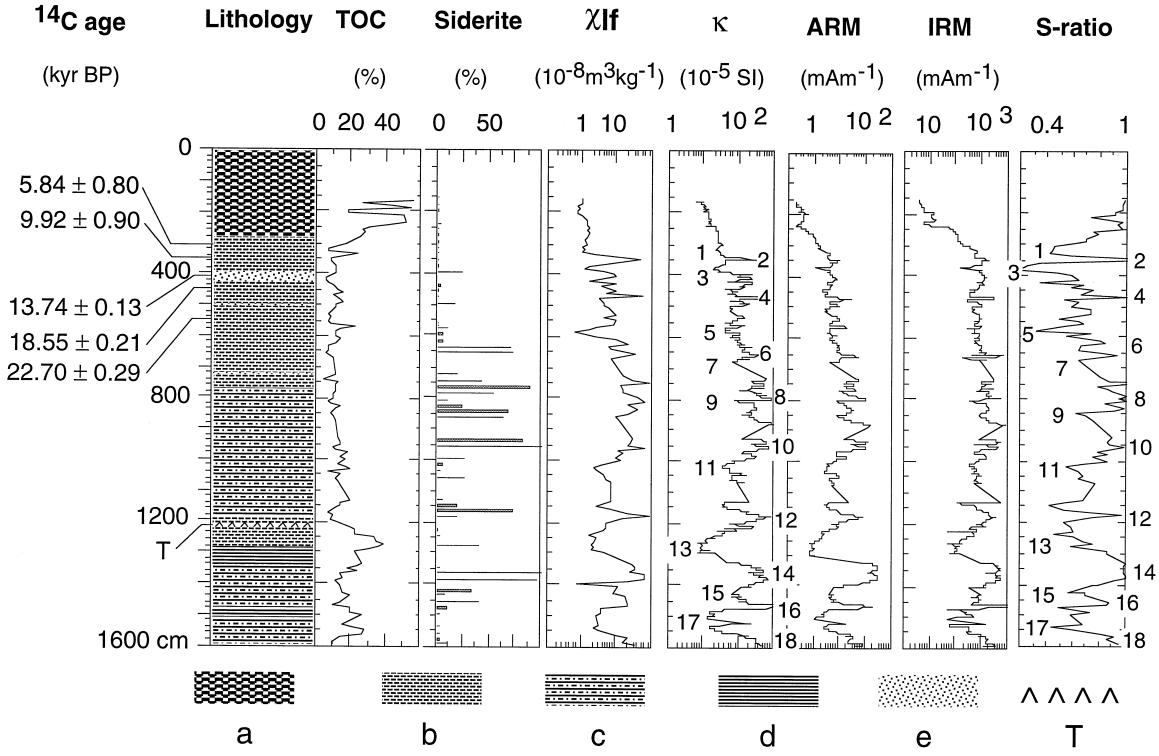

Fig. 3. Lithology (same symbols as shown in Fig. 2), AMS ^{14}C ages and profiles of TOC, siderite content (% of fraction > 63 μm), magnetic susceptibilities χ_{lf} and κ, ARM, IRM and *S*-ratio for core T-II. Numbers 1–18 indicate the main magnetic features of the T-II record (see text for explanation).

Table 1
AMS ^{14}C dates and corresponding calibrated calendar ages

Sample	Type	Depth in T-II (cm)	AMS ^{14}C age (yr BP)	σ (+/−)	Calibrated age (calendar yr BP)	Calibration method
LT/140 cm	macrophyte	156.6	2840	60	2948	dendro.
T-II/300 cm	macrophyte	300	5840	80	6648	dendro.
LT/345 cm	macrophyte	349	6290	110	7153	dendro.
LT/356.7 cm	macrophyte	349.4	8460	130	8412	dendro.
T-II/350 cm	macrophyte	350	9920	90	11153	dendro.
LT/379 cm	macrophyte	353.9	12750	170	14910	U/Th
T-II/411 cm	macrophyte	411	13740	130	16198	U/Th
LT/412 cm	macrophyte	424.9	15070	170	17847	U/Th
T-II/450 cm	charcoal	450	18550	210	21965	U/Th
LT/463 cm	macrophyte	457.4	19210	180	22736	U/Th
T-II/552 cm	charcoal	552	22700	290	26732	U/Th
LT/1300 cm	macrophyte	1316.6	36200	1200	40845	U/Th

2 on charcoals and 4 on bulk organic matter from cores LT and T-II. The four dates obtained from the bulk organic matter are biased by detrital organic particles [11], and were thus eliminated. The twelve valid ^{14}C dates indicate that the upper 13 m of the sequence were deposited since ~ 36 ^{14}C kyr BP (Table 1).

Facies (c) and (d) dominate the late Pleistocene sedimentary sequence and are indicative of periods of greater erosion. In some laminated parts of the record (especially between 6.5 and 10 m), lithological observations, mineral grain-counts and X-ray diffraction (XRD) indicate a relative enrichment in siderite ($FeCO_3$) and vivianite (iron phosphate) grains, which are typical of early diagenetic iron reduction processes in non-sulfidic lacustrine conditions [12] (Fig. 3).

5. Magnetic mineralogy

Thermomagnetic experiments, XRD and scanning electron microscope (SEM) analyses were performed on magnetic mineral concentrates. Magnetic grains were extracted by pumping a sediment slurry between the poles of an electromagnet which provides a 0.8 T dc field. This extraction procedure is usually successful in isolating the dominant ferrimagnetic minerals, including greigite or pyrrhotite, if present. The extracted material was dried and directly used for XRD (Philips PW 1710, Co radiation), SEM observations, and energy-dispersive X-ray (EDAX) analyses.

SEM observations and EDAX analyses of magnetic separates demonstrate the dominance of Al–Ti iron oxides as the main extracted minerals (Fig. 4). Al and Ti contents are relatively high (Table 2), which indicates a detrital origin for most extracted minerals. X-ray diffractograms of four magnetic concentrates indicate the presence of magnetite and hematite as the main extracted minerals. No magnetic iron sulfides were identified by SEM, EDAX or XRD methods.

Smoothed and rounded grains, as well as grains with dissolution pits, are commonly observed and suggest that iron oxide dissolution has occurred. This is not surprising, because the occurrence of siderite and vivianite concretions is associated with dissolution of iron oxides [12,13].

6. Mineral-magnetic behavior

Magnetic susceptibility, and anhysteretic and isothermal remanent magnetizations (ARM and IRM) were measured at 1 cm intervals on U-channel samples (results are in volume units). The magnetic susceptibility (κ) was measured on a Bartington Instruments MS-2 susceptibility meter. ARMs were imparted in a 50 μT bias field, superimposed on a 70 mT alternating field (Schonstedt GSD-1). The IRMs were introduced in a 0.5 T field. All remanences

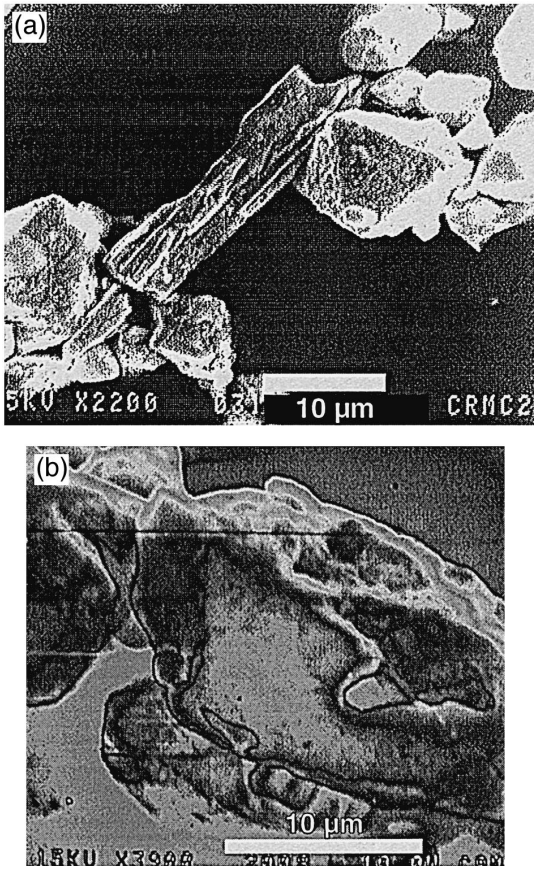

Fig. 4. SEM photomicrographs of magnetic separates: (a) characteristic octahedra of titano-magnetite or maghemite (Ti/Fe ≈ 0.3) from the watershed soil; and (b) characteristic iron oxide (Ti/Fe ≈ 0.46) from the lake sediment (core T-II, 900–1000 cm), showing a smoothed and rounded shape and several dissolution pits.

were measured using a 2 G, 3-axis, pass-through cryogenic magnetometer [14]. Hysteresis and backfield remanence curves were measured on ~50 mg dry samples by using a ''Micromag'' alternating gradient force magnetometer (Princeton Measurements Corporation), and the *S*-ratio ($-\mathrm{IRM}_{-0.3\,\mathrm{T}}/\mathrm{IRM}_{1\,\mathrm{T}}$) was calculated for each sample.

The main mineral-magnetic changes in the LT sedimentary sequence closely correspond to lithological changes (Figs. 2 and 3). Late Pleistocene silty clays are associated with high values of strongly concentration-dependent magnetic parameters such as κ, IRM or ARM. The effect of porosity and water content on the volume-normalized changes of κ, IRM or ARM was checked by comparing κ with the χ_{lf} of dried sediments, as determined from hysteresis data: both parameters generally indicate the same downcore changes with the same magnitude (Fig. 3), which indicates little contribution of the water content on the observed changes.

The upper Holocene peat (0–250 cm) is characterized by relatively low κ ($< 10^{-3}$ SI units), ARM ($< 5 \times 10^{-4}$ A m^{-1}) and IRM ($< 7 \times 10^{-3}$ A m^{-1}) values. High *S*-ratio values (> 0.9) and hysteresis parameters ($H_c < 11$ kA m^{-1}; $H_{cr}/H_c < 4$ and $M_r/M_s < 0.2$) indicate a low-coercivity magnetite-like signature (Figs. 2 and 3).

Late Pleistocene/early Holocene lacustrine silty clays (ca. 35 to 6 ^{14}C kyr BP) have higher κ values and contain more complex magnetic signatures, as shown on Fig. 3 for core T-II. *S*-ratio values, which range from 0.2 to 1, suggest important changes in the relative concentration of high-coercivity Fe(III) minerals such as hematite or goethite [15]. Lower *S*-ratio (< 0.7) and κ values ($< 10^{-3}$ SI) are observed at ca. 300–380, 550–600, 1000–1280 and 1370–1540 cm. These zones likely correspond to enrichments in high-coercivity Fe(III)-oxide phases.

The higher κ ($> 5 \times 10^{-3}$ SI) values from the remainder of the record are generally associated with high *S*-ratio values (> 0.9). The corresponding laminated sediments are enriched in authigenic siderite

Table 2
EDAX probe analyses of magnetically extracted minerals

		Fe/(Fe + Ti + Al)	Ti/(Fe + Ti + Al)	Al/(Fe + Ti + Al)
Present-day soil	mean ($n = 8$)	0.63	0.13	0.24
	σ	0.16	0.08	0.16
Core T-II	mean ($n = 5$)	0.64	0.16	0.20
900-1000 cm	σ	0.07	0.11	0.06

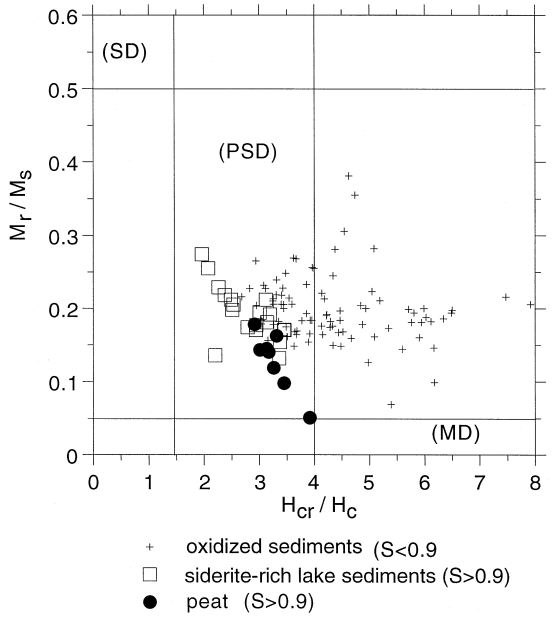

Fig. 5. Binary plot of M_r/M_s and H_{cr}/H_c. Data are from peats (*black dots*), laminated siderite-rich sediments (*open squares*) and oxic lacustrine sediments (*crosses*). *SD* = single domain; *PSD* = pseudo-single domain; *MD* = multi-domain, after Day et al. [16].

and vivianite, especially between 1000 and 650 cm (Fig. 3). This suggests a relative absence of high-coercivity Fe(III)-oxides in sediments that are affected by reductive diagenesis.

As primarily suggested by the distribution of *S*-ratio values with depth, hysteresis parameters M_r/M_s and H_{cr}/H_c [16] indicate two types of magnetic mineral assemblages (Fig. 5). The Holocene peats and the siderite-rich sediments contain magnetic assemblages that are probably dominated by PSD to MD (titano-)magnetite. The second type of assemblage is characterized by higher coercivities (and lower *S*-ratio values) from sediments that are enriched in ferric iron oxides (oxidized magnetites, hematite or goethite).

κ, χ_{lf}, IRM, ARM and M_s are strongly dependent on the relative concentration of strongly ferrimagnetic phases like magnetite or maghemite. Additional ferrimagnetic grain size effects may covary with magnetic susceptibility, ARM and IRM, but they have no effect on M_s.

The relatively high values of magnetic susceptibility and remanences in terrigenous silty clays suggest a strong relation between erosional processes and magnetic concentration of detrital (titano-)magnetite. This relationship is explained by the dilution of ferrimagnetic terrigenous components by diamagnetic biogenic components (e.g., organic matter or biogenic silica), as illustrated by oppositely correlated changes in TOC and magnetic concentration proxies (Figs. 2 and 3). The association between ferromagnetic concentration and terrigenous inputs could also be magnified by changes of the mineralogy of iron oxides. As shown in Fig. 6, plots of κ vs. *S*-ratio and M_s vs. H_{cr} clearly indicate that low-coercivity (titano-)magnetite-bearing sediments correspond either to peaty sediments with low κ and M_s or to laminated lacustrine silty clays with high κ and M_s. In contrast, high-coercivity hematite- or goethite-bearing sediments generally correspond to intermediate κ and M_s values.

Because κ and M_s values are respectively $\sim$1000 and $\sim$200 times higher for magnetite than for hematite, the low-temperature oxidation of magnetite into Fe(III)-(oxyhydr)oxides will decrease these parameters to lower values. At Lake Tritrivakely, the primary detrital fraction is enriched in Fe(III)-oxides from well-developed oxisols (e.g., [17]). For example, *S*-ratio values from present-day soils do not exceed 0.85, a value which indicates at least 80% of hematite in experimental magnetite–hematite mixtures [18]. The high coercivity of LT sediments thus indicates the occurrence of oxic depositional environments which allow the relative preservation of Fe(III)-oxides. In contrast, given the detrital origin of Ti–Al magnetic oxides, the absence of a significant high-coercivity component in the LT Holocene peat or in laminated siderite-rich sediments (*S*-ratio > 0.9) likely reflects the dissolution of Fe(III)-oxides. Theoretical and experimental studies [19–21] and observations of lake sediments [13] show that iron reduction processes under anoxic conditions result in the dissolution of ferrimagnetic iron oxides, primarily Fe(III)-bearing particles such as goethite and hematite. In present-day eutrophic and peaty environments, dissolution processes are strong enough to remove most of the ferrimagnetic iron oxides from the sediment [22]. This produces very low values of κ and M_s, as observed in the LT *Cyperaceae* peat.

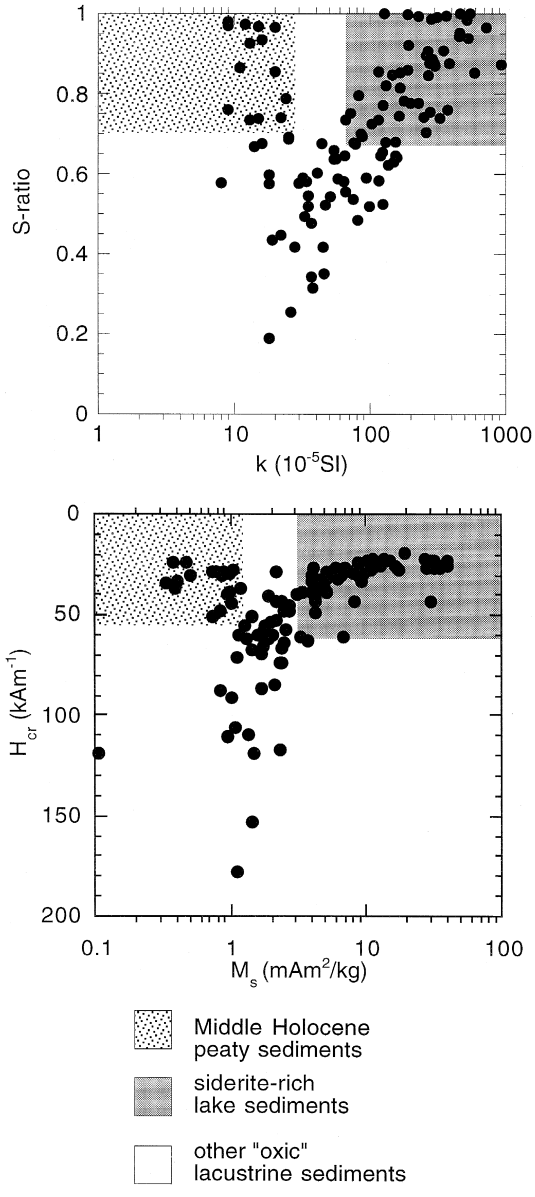

Fig. 6. Binary plot of *S*-ratio vs. κ and H_{cr} vs. M_s (see text for explanation).

In non-sulfidic depositional environments from freshwater lakes, early diagenetic processes proceed rapidly to the anaerobic reduction of iron oxides and oxidation of organic matter. This results in high concentrations of dissolved Fe(II) and CO_2 which cause supersaturation of siderite [23,24]. Siderite formation is favoured by strong terrigenous inputs which lead to the rapid burial of detrital iron and degradable organic matter [13]. Low-coercivity siderite-rich and laminated sediments in Lake Tritrivakely (e.g., between 6.5 and 10 m) have high relative κ or M_s values, which is consistent with freshwater meromictic environments and relatively high terrigenous input. Such environments are thus highly favorable to the dissolution of high-coercivity-Fe(III) iron (oxyhydr)oxides.

On the basis of the above results, the LT mineral-magnetic records likely reflect changes between three environmental end-members (Fig. 6) which constrain the concentration and mineralogy of iron oxides in the sediment:

(1) In Holocene peats, detrital iron oxides have been diluted by diamagnetic organic matter and have been dissolved under reducing conditions. The resulting sediments contain PSD-magnetite with low κ ($< 10^{-4}$ SI) and M_s (< 1 mA m^2 kg^{-1}) values.

(2) In slowly deposited ''oxic'' sediments from ephemeral shallow-water environments, detrital ferric oxides have been relatively preserved, resulting in high H_{cr}/H_c values (> 4) and low *S*-ratios (< 0.9), with intermediate κ ($> 10^{-4}$ SI) and M_s (> 1 mA m^2 kg^{-1}) values.

(3) In anoxic siderite-rich laminated sediments from permanent freshwater and meromictic environments [10], relatively strong erosional processes resulted in the rapid burial of organic matter and high concentrations of detrital iron-bearing minerals which favoured the dissolution of ferric (high coercivity) iron oxides and the precipitation of authigenic siderite.

The resulting sediments contain relatively high concentrations of magnetite and they have high κ ($> 10^{-3}$ SI) and M_s (> 10 mA m^2 kg^{-1}) values.

As shown in Fig. 3, nine ''high coercivity/low susceptibility'' zones indicate periods of oxic conditions and low terrigenous inputs in the sedimentary record from core T-II (odd numbers). In contrast, nine ''low coercivity/high susceptibility'' (even numbers) zones indicate periods of increased dissolution and erosion in meromictic environments. These results suggest a marked instability of the lacustrine environment throughout the late Quaternary.

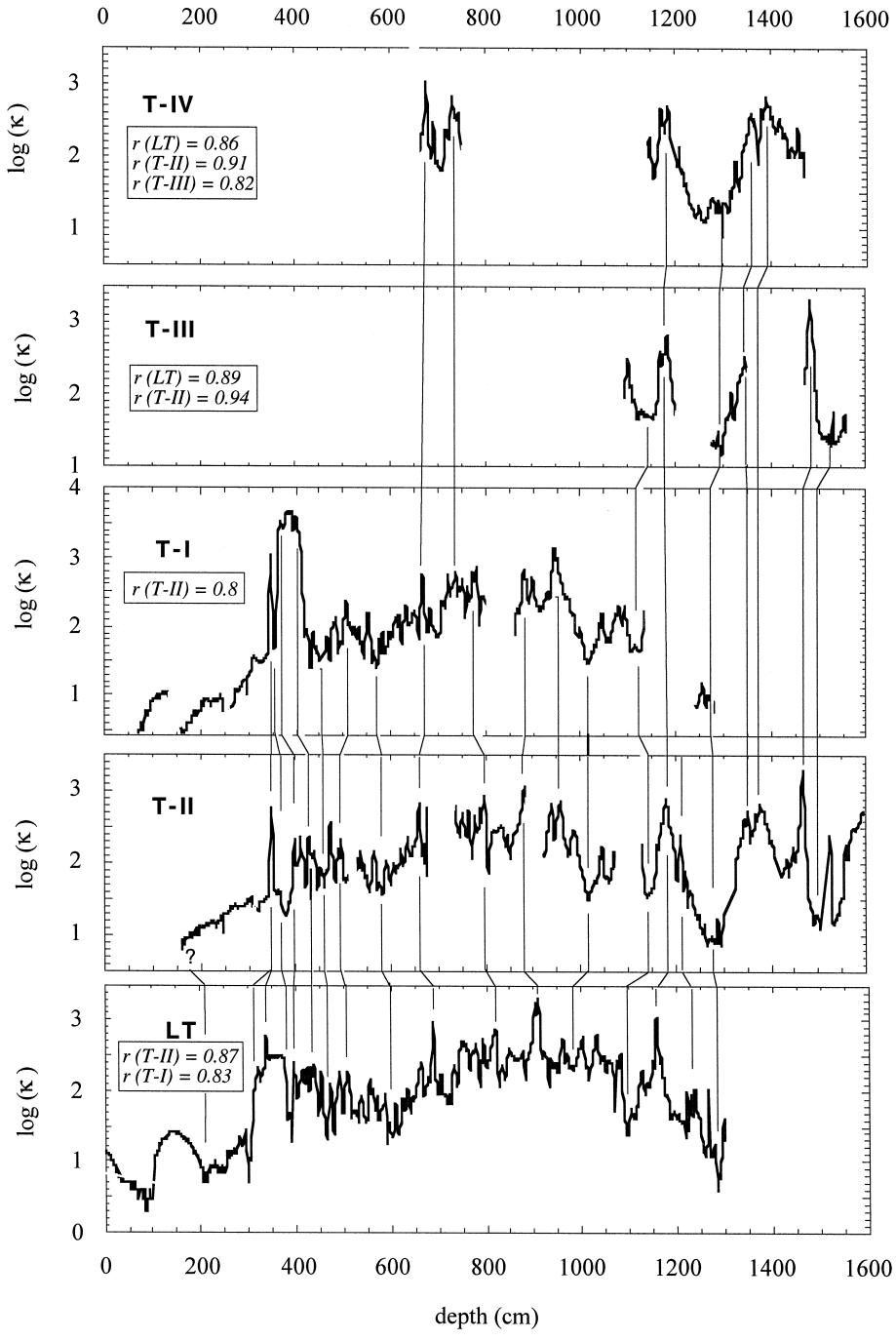

Fig. 7. The five κ records from the Lake Tritrivakely cores (LT, T-I, T-II, T-III and T-IV). Cores T-III and T-IV only recover some missing intervals from the other cores. A common depth-scale, based on core T-II, was determined after correlation of the different profiles. Also shown are the correlation coefficients (r) between the respective sets of κ data.

7. Correlation of cores and age model

Correlation of the five sediment cores was achieved with the respective κ profiles (Fig. 7). Characteristic features from each profile were easily identified (from 16 to $\sim$4 m). The upper part of the record (from $\sim$4 to 0 m) was more difficult to correlate, probably because of significant spatial variability of deposition in this depth (time) interval. We performed the inter-core correlation by using software [25] which allows calculation of correlation coefficients between two sets of core data.

Core T-II was chosen as the ''master core'' because it contains the longest sequence. All of the data (κ records of cores LT, T-I, T-III and T-IV, pollen records and ^{14}C ages from core LT) were then transferred to the core T-II depth scale by using a linear function between two successive control points from the correlated magnetic susceptibility records.

A time-scale was established by using the AMS ^{14}C dates from macrophyte debris and charcoal. These ^{14}C dates were converted to calendar ages (Table 1; Fig. 8) by using the calibration curves of the German oak and pine tree-ring records down to 10,000 ^{14}C yr BP [26,27]. Between 18,000 and 10,000 ^{14}C yr BP, we used the linear equation of Bard et al. [28], as obtained from the coupling of ^{14}C and uranium series measurements on the same corals:

$$\text{calendar age} = 1.24(^{14}\text{C conventional date}) - 840$$

Beyond 18,000 ^{14}C yr BP, conversion of our ^{14}C ages to calendar ages was performed using the following equation (E. Bard, pers. commun.):

$$\text{calendar age} = -5.85 \times 10^{-6}(^{14}\text{C conv. date})^2 + 1.39(^{14}\text{C conv. date}) - 1807$$

Although this equation is based on only two pairs of U/Th–^{14}C measurements older than 22 kyr, it is our best estimate for the chronology of the LT deposits.

The core T-II depth scale was converted into a time-scale by assuming constant accumulation rates between two successive calibrated ages. The resulting depth–age profile indicates variable deposition rates, with intermediate to high values (0.3–0.9 mm/yr). Dramatic decreases in apparent deposition rate ($<$0.1 mm/yr) are suggested for core T-II between 455 and 411 cm ($\sim$22 and 16 kyr) and at $\sim$350 cm (between $\sim$15 and 7 kyr), which is probably indicative of discontinuous sedimentation and erosion in these oxidized (low *S*-ratio) depth-intervals.

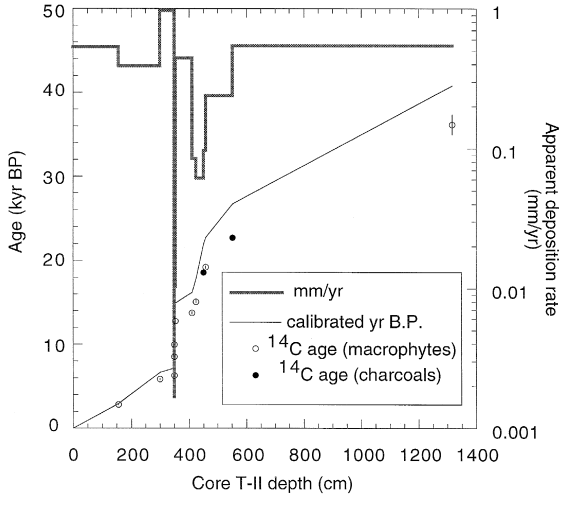

Fig. 8. Core T-II age vs. depth profile after correction of the ^{14}C ages to calendar ages. Also shown is the apparent deposition rate (*heavy line*).

8. Environmental change during the last 46 kyr

κ (stacked) and *S*-ratio are shown versus age in Fig. 9 with TOC [29], *Cyperaceae* and *Ericaceae* pollen percentages [10]. The stacked κ record was obtained by averaging all the susceptibility values at 200 yr time intervals (as projected on the T-II depth scale).

The bottom part of the record (before $\sim$35 kyr) contains relatively high *Ericaceae* pollen percentages, indicating steppe-like conditions on the watershed. This period contains high-amplitude changes in TOC and magnetic properties: three low κ/low *S*-ratio events suggest low detrital input and shallow/oxic environments at ca. 45.3–42.6, 40–39 and 37.8–35 kyr, respectively. The corresponding high TOC percentages ($>$20%) are associated with increased input of autochthonous organic matter [29]. In the remaining part of this section, higher κ and *S*-ratios indicate stronger runoff intervals and suggest increased Fe(III)-(oxyhydr)oxide dissolution in anoxic environments. Similarly high κ, high *S*-ratios

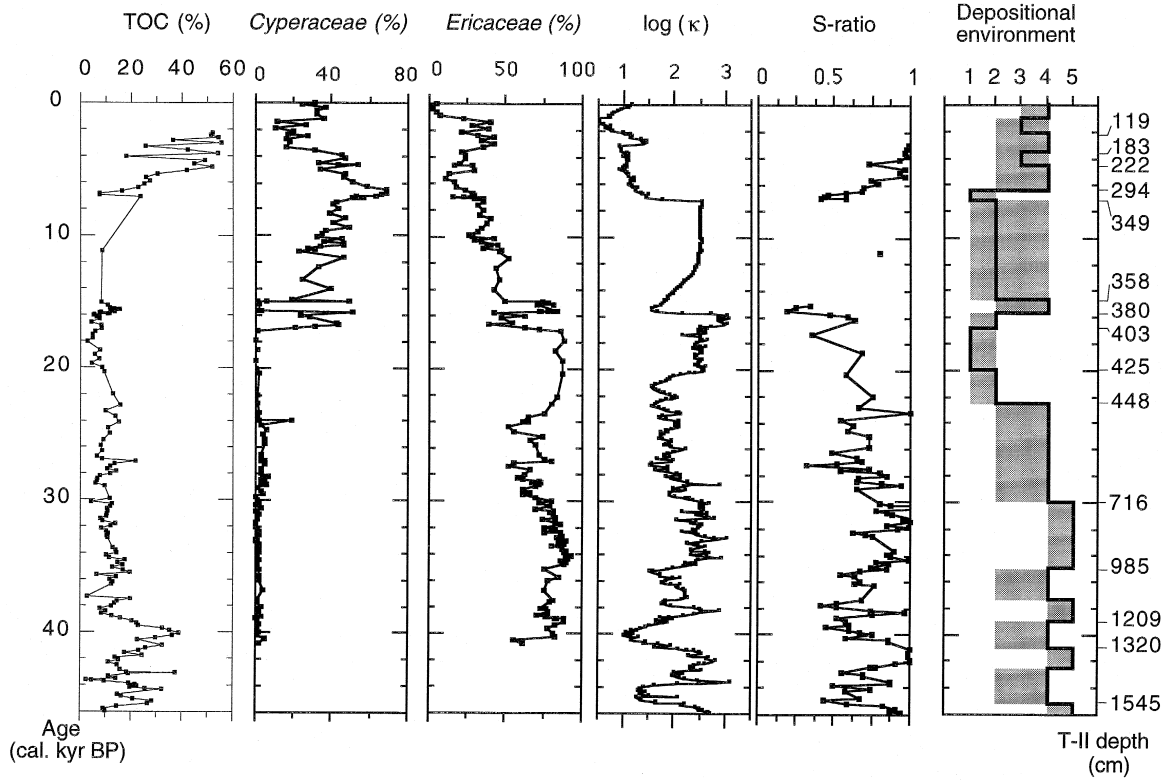

Fig. 9. The Lake Tritrivakely paleoenvironmental proxies plotted with respect to age [TOC, *Cyperaceae* and *Ericaceae* pollen percentages, stacked magnetic susceptibility (κ, interpolation: 200 yr), *S*-ratio] and interpreted depositional environment (*solid line*) with estimated uncertainty (*shaded area*). *1* = oxic environment, discontinuous deposition; *2* = oxic environment, ephemeral swamp; *3* = peat-bog; *4* = permanent swamp–shallow lake; *5* = meromictic lake.

and siderite content between ca. 35 and 30 kyr indicate that detrital input and associated early diagenetic processes dominate the paleoenvironmental record. Evidence for greater runoff is also provided by the increase in allochthonous organic matter [29]. The high percentages of *Ericaceae* pollen suggest that cold conditions and steppe-like vegetation existed in this interval.

Between ca. 30 and 22.5 kyr, the general decrease of κ and the spell of low *S*-ratios events at ca. 29, 27 and 24 kyr document oxic conditions and the weakening of runoff and iron oxide dissolution. Warmer and drier conditions were also suggested by the respective decrease in *Ericaceae* pollen, and the increase in organic matter (TOC > 10%) derived from subaquatic macrophytes [29].

From ~22.5 kyr, the LT paleoenvironmental record contains more complex changes. A significant drop in apparent deposition rate (from ~0.5 mm/yr before 22 kyr to less than ~0.1 mm/yr at ~16 kyr) strongly suggests that deposition was discontinuous during the Last Glacial Maximum. This is also suggested by the persistence of high-coercivity detrital magnetic assemblages (*S*-ratio < 0.65) which indicate oxic/shallow water depositional environments. Between ca. 22 and 17 kyr, an *Ericaceae* pollen maximum (> 70% of the pollen taxa) suggests very cold conditions. Progressive increases in the silty fraction [10] and magnetic susceptibility ($\kappa > 3.10^{-3}$ SI) from 20 kyr indicate increasing contributions of the terrigenous components. These relatively ephemeral and shallow/oxic depositional environments seem to culminate between and 17 and 16 kyr, as documented by maximum susceptibility values ($> 10^{-2}$ SI), low *S*-ratio (< 0.7) and minimum TOC content (~4%). Low apparent deposition

rates (<0.1 mm/yr; Fig. 8) suggest that deposition was not continuous and that erosion may have occurred during drier sub-events. The abrupt increase of *Cyperaceae* in this interval indicates the development of subaquatic vegetation on the lakeshores.

From ca. 16 to 15 kyr, an abrupt increase in *Ericaceae* suggests the occurrence of a cold and wet climatic event. The corresponding low κ values ($<5.10^{-4}$ SI) reflect dilution of terrigenous inputs by biogenic components [10]. The calculated deposition rate (~ 0.5 mm/yr) is consistent with near-continuous deposition, although the persistence of high-coercivity phases (S-ratio < 0.7) indicates oxic environments during this period.

The late Pleistocene/Holocene transition at Lake Tritrivakely is defined by strong lateral changes of condensed deposition between ca. 15 and 7.2 kyr. *Ericaceae* percentages decrease progressively and reflect a large and general warming, as expected. This time-interval is only covered by 5 cm thick oxidized clayey sediments in cores T-II or T-1, and a similar 31 cm thick layer in core LT. The three calibrated ages from this interval in core LT indicate very low deposition rates (<0.01 mm/yr). This could be explained by the occurrence of several hiatuses of short, but undetermined, duration. Core LT sediments with high κ values ($>5.10^{-3}$ SI) indicate a strong terrigenous contribution. The diatom flora indicate the occurrence of circumneutral swamps which tend to evolve toward an acidic bog between 8.1 and 6.4 kyr [10]. As shown by extremely low S-ratio values (<0.5), oxic environments seem to culminate around 7 kyr.

The middle to late Holocene period is characterized by the dominance of peaty environments [9], with high TOC values ($>20\%$) and high *Cyperaceae* pollen percentages ($>40\%$). The low magnetic susceptibilities ($\kappa < 5.10^{-4}$ SI) and PSD-like hysteresis behavior ($H_{cr}/H_c \approx 3$; $M_r/M_s \approx 0.15$) of these peats result from: (1) dilution of terrigenous inputs by dominant organic components ($>50\%$ of the dry sediment); and (2) from dissolution of iron oxides in reducing and acidic conditions [22].

Between ca. 3.6 and 2.2 kyr, a peak of magnetic susceptibility (culminating at 3 kyr) documents a short runoff event, possibly associated with cooler conditions, as suggested by an *Ericaceae* increase (up to 40% of the pollen taxa).

Although the data indicate that peat-bog environments prevailed during the last 2.2 kyr, significant increases in diatom concentrations and strong changes in the composition of organic debris [29] suggest relatively more open-water environments during the last millennium.

9. Comparison with other regional data

From ~ 46 to 20 kyr, Lake Tritrivakely experienced periods of positive water balance which led to the establishment of a permanent lake from ~ 39 to ~ 30 kyr. Quantitative temperature estimates from palynological data in Equatorial Africa [30] inferred conditions cooler than present for the last glacial period (-3 ± 1.9°C).The transfer of our time-scale to other sites, pollen and lacustrine records from Saltpan (SP) in South Africa [31] and from speleothems in Botswana (CC) and South Africa (LOB) [32,33] indicate warm and wet climates around ~ 44 kyr, moderately cool and dry conditions prior to ~ 35 kyr, and dry conditions until the mid-Holo-

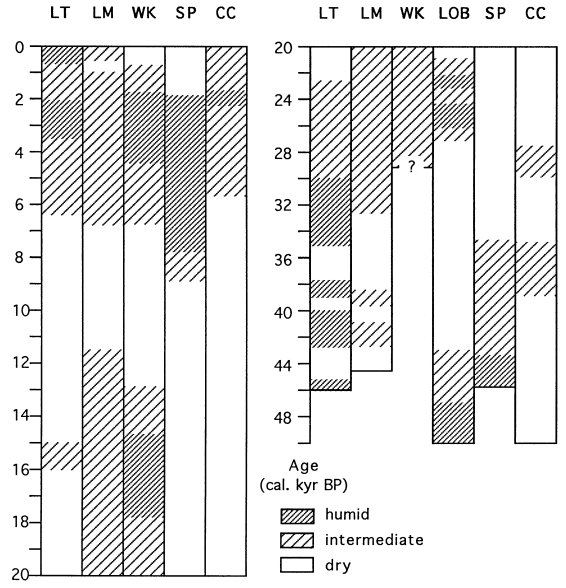

Fig. 10. A comparison of the Lake Tritrivakely paleoenvironmental record with other paleoclimate proxies from southeast Africa (see Fig. 1). *LT* = Lake Tritrivakely, 19°47′S (this study); *LM* = Lake Malawi, 9°30′S [34]; *WK* = Wonderkrater, 24°26′S [35]; *SP* = Saltpan, 25°34′S [31]; *LOB* = Lobatse, 25°30′S [33]; *CC* = Cango Caves, 34°S [32].

cene (Fig. 10). No evidence for wet conditions is found in this region between 35 and 32 kyr.

The tendency toward drier conditions in LT from 30 kyr contrasts with the onset of a humid period which lasted until ca. 11.5 and 13 kyr in Lake Malawi (LM) (14°30′S) [34] and in Wonderkrater (WK) (24°30′S) [35], respectively. At the end of this dry period (especially between 22 and 17 kyr), our data document the existence of an ephemeral swamp in LT. This time-interval falls in the coldest period in the region, and coincides with one of the major advances of mountain glaciers (~18–16.5 kyr) in the Southern Hemisphere [36,37].

Between ca. 17 and 7 kyr, our data indicate discontinuous deposition and oxic ephemeral water bodies, especially from 15 kyr. In contrast, relatively humid conditions persisted in southeast Africa before ~12 kyr [34,35], suggesting that there is no straightforward evidence for a widespread aridity south of 8°S in East Africa before ~12 kyr. The age of 15 kyr closely matches with the major sea-ice retreat from the North Atlantic [38]. Neither the abrupt decrease in aridity over the Southern Hemisphere at 14.6 kyr [39] nor the strong increase of moisture over Equatorial Africa after 10 kyr [40] are observed in the LT record. Warm and dry conditions in the Ankaratra mountains persisted until ~7 kyr, at the end of the early to mid-Holocene climatic transition [43]. From ~7 kyr, the Holocene continental glaciers retreated in South Georgia Island [44] and the warmest estimated air-temperatures in Antarctica occurred [45].

In southeast Africa, the advent of moister conditions seem to have occurred from ~7.8 kyr, likely reflecting the orbitally induced increase of summer insolation over the Southern Hemisphere [40]. A greater proportion of summer rainfall is suggested in this region from ~5.8 kyr, especially between ca. 3.8 and 2.6 kyr [41,42].

The LT middle to late Holocene record consists of shallow peat-bog environments, whereas open-water conditions and increased runoff probably occurred between 3.6 and 2.2 kyr and for the last millennium during cooler periods.

Our observations point out characteristic features of the lacustrine dynamics at Lake Tritrivakely. Except for the interval ca. 23–17 kyr, shallow/oxic and ephemeral environments generally dominated during relatively warm periods (as observed in the middle Holocene), whereas permanent/anoxic lacustrine environments occurred during relatively cold periods of increased runoff such as during the ca. 35–23 kyr period. As observed today in the Madagascar highlands, past water budgets were probably highly constrained by temperature changes through evaporation processes. These LT results contrast with numerous sites located in the actual summer rainfall area from southeast tropical Africa, which experienced drier conditions before 30 kyr and wetter conditions between 23 and 10 kyr and from 7 kyr. Such differences could be associated with the pattern of atmospheric circulations in the Mozambique channel and with the activation of the Agulhas Current during interglacial periods [46]. Present-day climatic observations and models [42,47] show that wet spells in the summer rainfall area of South Africa are linked to a strong Agulhas Current. In contrast, during dry spells, the flow of the Agulhas Current decreases and the summer convergence cells shift eastward, preferentially over the Indian Ocean and Madagascar. Such apparent zonal shifts of the intertropical convergence may possibly explain the variability of water balance records observed between Madagascar and East Tropical Africa.

10. Conclusions

The mineral-magnetic properties of Tritrivakely maar-lake sediments are strongly controlled by erosional processes and early diagenesis of iron-bearing minerals in non-sulfidic conditions. High-coercivity ferric (oxyhydr)oxides are preserved during dry periods of low lake-level. In contrast, the high-coercivity component is absent in the siderite-rich laminated sediments which relate to permanent and stratified water bodies. Although further work is needed to detail the relationships between the early diagenesis of magnetic iron oxides and erosional processes in such maar lake environments, a detailed late Quaternary paleoenvironmental record in the Ankaratra mountains was provided by comparing mineral-magnetic parameters to other paleoenvironmental proxies along a ^{14}C calibrated timescale. Significant variability of the depositional environment was observed for the last 46 kyr. Permanent water bodies prevailed

before 22 kyr, while ephemeral swamp or peat-bog environments developed during the Last Glacial Maximum and after 7 kyr.

As a consequence, contrasted water balance records are inferred between the summer rainfall region of Madagascar and the summer rainfall region of southeast Africa for the Late Glacial and the Holocene. Further studies are required to develop a better understanding of such contrasts, which suggest zonal changes of the tropical convergence on the western side of the Indian Ocean.

Acknowledgements

We are pleased to acknowledge L. Ferry, J.L. Saos and the Office de Recherches Scientifiques et Techniques d'Outre-Mer (ORSTOM), and the University of Tananarive for their helpful contribution to field operations, and E. Bard for providing unpublished data. Many thanks to Bernie A. Housen (Western Washington University), Andrew P. Roberts (University of Southampton) and John Peck for their help during the preparation of this paper. This work is a contribution of GDR 970 of the Centre National de la Recherche Scientifique. *[RV]*

References

[1] K.L. Verosub, A.P. Roberts, Environmental magnetism: Past, present, and future, J. Geophys. Res. 100 (1995) 2175–2192.
[2] R.L. Reynolds, J.W. King, Magnetic records of climate change, in: U.S. National Report to International Union of Geodesy and Geophysics 1991–1994), Rev. Geophys. Suppl. (1995) 101–110.
[3] N. Thouveny, J.L. de Beaulieu, E. Bonifay, K.M. Creer, J. Guiot, J. Icole, S. Johnsen, J. Jouzel, M. Reille, T. Williams, D. Williamson, Climate variations in Europe over the past 140 kyr deduced from rock magnetism, Nature (London) 371 (1994) 503–506.
[4] N. Thouveny, D. Williamson, Palaeomagnetic study of the Holocene and upper Pleistocene sediments from lake Barombi Mbo, Cameroun: first results, Phys. Earth Planet. Inter. 52 (1988) 193–206.
[5] D. Williamson, N. Thouveny, C. Hillaire-Marcel, A. Mondeguer, M. Taieb, M. Tiercelin, A. Vincens, Chronological potential of geomagnetic oscillations recorded in Late Quaternary sediments from Lake Tanganyika, Quat. Sci. Rev. 10 (1991) 1–12.
[6] D. Williamson, M. Taieb, B. Damnati, M. Icole, N. Thouveny, Equatorial extension of the Younger Dryas event: rock-magnetic evidence from Lake Magadi, Global Planet. Change 7 (1993) 235–242.
[7] P. Segalen, Étude des sols dérivés de roches volcaniques basiques à Madagascar, Mém. IRSM D (1957) 1–182.
[8] F. Bourgeat, Contribution à l'étude des sols sur socle ancien à Madagascar. Types de différenciation et interprétation chronologique au cours du Quaternaire, Doctorat de Sciences Naturelles, 1970.
[9] D.A. Burney, Pre-settlement vegetational change at Lake Tritrivakely Madagascar, Palaeoecol. Afr. 18 (1987) 357–381.
[10] F. Gasse, E. Cortijo, J.R. Disnar, L. Ferry, E. Gibert, C. Kissel, F. Laggoun-Defarge, E. Lallier-Vergés, J.C. Miskovsky, B. Ratzimbazafy, F. Ranaivo, L. Robison, P. Tucholka, J.L. Saos, A. Siffedine, M. Taieb, E. Van Campo, D. Williamson, A 36 ka environmental record in the southern tropics: Lake Tritrivakely (Madagascar), C.R. Acad. Sci., Paris 318 (1994) 1513–1519.
[11] D. Burney, Late Quaternary stratigraphic charcoal records from Madagascar, Quat. Res. 28 (1987) 274–280.
[12] R.A. Berner, A new geochemical classification of sedimentary environments, J. Sediment. Petrol. 51 (1981) 359–365.
[13] C. Curtis, Mineralogical consequences of organic matter degradation in sediments: Inorganic/organic diagenesis, in: J.K. Legett (Ed.), Marine Clastic Sedimentology, G.G.Z. Graham and Trotman, London, 1987, pp. 108–123.
[14] R. Weeks, C. Laj, L. Endignoux, M. Fuller, A. Roberts, R. Manganne, E. Blanchard, W. Goree, Improvements in long-core measurement techniques: Applications in palaeomagnetism and palaeoceanography, Geophys. J. Int. 114 (3) (1993) 651–663.
[15] A.J. van Velzen, D.A. Zijderveld, Effects of weathering on single-domain magnetite in Early Pliocene marine marls, Geophys. J. Int. 121 (1995) 267–278.
[16] R. Day, M. Fuller, V.A. Schmidt, Hysteresis properties of titanomagnetites: grain size and compositional dependance, Phys. Earth Planet Inter. 13 (1977) 260–267.
[17] J.E.M. Allan, J.M.D. Coey, M. Resende, J.D. Fabris, Magnetic properties of iron-rich oxisols, Phys. Chem. Miner. 15 (1988) 470–475.
[18] J. Bloemendal, J.W. King, A. Hunt, P.B. DeMenocal, A. Hayashida, Origin of the sedimentary magnetic record at Ocean Drilling Program sites on the Owen Ridge, Western Arabian Sea, J. Geophys. Res. 98 (1993) 4199–4219.
[19] D.E. Canfield, R.A. Berner, Dissolution and pyritization of magnetite in anoxic marine sediments, Geochim. Cosmochim. Acta 51 (1987) 645–659.
[20] D.E. Canfield, R. Raiswell, S. Bottrell, The reactivity of sedimentary iron minerals toward sulfide, Am. J. Sci. 292 (1992) 659–683.
[21] J. Bruno, W. Stumm, P. Wersin, F. Branberg, On the influence of carbonate in mineral dissolution: I. The thermodynamics and kinetics of hematite dissolution in bicarbonate solutions at $T = 25°C$, Geochim. Cosmochim. Acta 56 (1992) 1139–1147.
[22] M. Williams, Evidence for the dissolution of magnetite in recent Scottish peats, Quat. Res. 37 (1992) 171–182.

[23] S. Emerson, Early diagenesis in anaerobic lake sediments: chemical equilibria in interstitial waters, Geochim. Cosmochim. Acta 40 (1976) 925–934.
[24] J. Bruno, P. Wersin, W. Stumm, On the influence of carbonate in mineral dissolution: II. The solubility of $FeCO_3$ (s) at 25°C and 1 atm total pressure, Geochim. Cosmochim. Acta 56 (1992) 1149–1155.
[25] D. Paillard, Modéles simplifiés pour l'étude de la variabilité de la circulation thermohaline au cours des cycles glaciaire–interglaciaire, Doctorat, Université Paris-Sud, Orsay, 1995.
[26] M. Stuiver, R.S. Kra, Calibration issue, in: M. Stuiver, R.S. Kra (Eds.), Proceedings of the 12th International ^{14}C Conference, Radiocarbon 28 (1986) 805–1030.
[27] B. Kromer, B. Becker, German oak and pine ^{14}C calibration, 7200–9439 BC, Radiocarbon 35 (1993) 125–135.
[28] E. Bard, M. Arnold, R.G. Fairbanks, B. Hamelin, $^{230}Th-^{234}U$ and ^{14}C ages obtained by mass spectrometry on corals, Radiocarbon 35 (1993) 191–199.
[29] A. Siffedine, F. Laggoun-Defarge, E. Lallier-Vergès, J.R. Disnars, D. Williamson, F. Gasse, E. Gibert, La sédimentation organique lacustre en zone tropicale sud au cours des 36 000 dernières années (Lac Tritrivakely, Madagascar), C.R. Acad. Sci., Paris 321 (1995) 385–391.
[30] R. Bonnefille, F. Chali, J. Guiot, A. Vincens, Quantitative estimates of full glacial temperatures in equatorial Africa from palynological data, Climate Dyn. 6 (1992) 251–257.
[31] T. Partridge, S.J. Kerr, S.E. Metcalfe, L. Scott, A.S. Talma, J.C. Vogel, The Pretoria saltpan: a 200,000 year southern African lacustrine sequence, Palaeogeogr., Palaeoclimatol., Palaeoecol. 101 (1993) 317–337.
[32] A.S. Talma, J.C. Vogel, Late Quaternary paleotemperatures derived from a speleothem from Cango Caves Cape Province, South Africa, Quat. Res. 37 (1992) 203–213.
[33] K. Holmgren, W. Karlen, P.A. Shaw, Paleoclimatic significance of the stable isotopic composition and petrology of a Late Pleistocene stalagmite from Botswana, Quat. Res. 43 (1995) 320–328.
[34] B.P. Finney, C.A. Scholz, T.C. Johnson, S. Trumbore, Late Quaternary lake-level changes of Lake Malawi, in: T.C. Johnson, E.O. Odada (Eds.), The Limnology, Climatology and Paleoclimatology of the East African Lakes, Gordon and Breach, London, 1995, pp. 495–508.
[35] L. Scott, A late Quaternary pollen record from the Transvaal Bushveld, South Africa, Quat. Res. 17 (1982) 339–370.
[36] E. Van Campo, J.C. Duplessy, W.L. Prell, N. Baratt, R. Sabatier, Comparison of terrestrial and marine temperature estimates for the past 135 kyr off southeast Africa: a test for GCM simulations of palaeoclimate, Nature (London) 348 (1990) 209–212.
[37] T.V. Lowell, C.J. Heusser, B.G. Andersen, P.I. Moreno, A. Hauser, L.E. Heusser, C. SchlŸchter, D.R. MarchantT, G.H. Denton, Interhemispheric correlation of Late Pleistocene glacial events, Science 269 (1995) 1541–1549.
[38] R.G. Fairbanks, A 17,000 year glaco-eustatic sea level record: influence of glacial melting rates on the Younger Dryas event and deep-ocean circulation, Nature (London) 342 (1989) 637–642.
[39] J. Jouzel, R. Vaikmaie, J.R. Petit, M. Martin, Y. Duclos, M. Stievenard, C. Lorius, M. Toots, M.A. Melieres, L.H. Burckle, N.I. Barkov, V.M. Kotlyakov, The two-step shape and timing of the last deglaciation in Antarctica, Climate Dyn. 11 (1995) 151–161.
[40] F.A. Street-Perrott, R.A. Perrott, Holocene vegetation, Lake-Levels and Climate of Africa, in: H.E. Wright, J.E. Kutzbach, T. Webb III, W.F. Ruddiman, F.A. Street-Perrott, P.J. Bartlein (Eds.), Global Climates Since the Last Glacial Maximum, University of Minnesota Press, Minneapolis, MN, 1993, pp. 318–356.
[41] L. Scott, Palynological evidence for Late Quaternary warming episodes in southern Africa, Palaeogeogr., Palaeoclimatol., Palaeoecol. 101 (1993) 229–235.
[42] A.L. Cohen, P.D. Tyson, Sea-surface temperature fluctuations during the Holocene off the south coast of Africa: implications for terrestrial climate and rainfall, Holocene 5 (1995) 304–312.
[43] J.C. Stager, P.A. Mayewski, Abrupt early to mid-Holocene climatic transition registered at the Equator and the poles, Science 276 (1997) 1834–1836.
[44] C.M. Clapperton, D.E. Sugden, J. Birnie, M.J. Wilson, Late-glacial and Holocene glacier fluctuations and environmental change on South Georgia, Southern Ocean, Quat. Res. 31 (1989) 210–228.
[45] C. Lorius, L. Merlivat, L. Jouzel, M. Pourchet, A 30,000-yr isotope climatic record from Antarctic ice, Nature (London) 280 (1979) 644–648.
[46] E. Vincent, Climatic change at the Pleistocene–Holocene boundary in the southwestern Indian Ocean, Palaeoecol. Afr. 6 (1972) 45–54.
[47] M.J. Cockroft, M.J. Wilkinson, P.D. Tyson, The application of a present-day climatic model to the Late Quaternary in Southern Africa, Climate Change 10 (1987) 161–181.